Preparation, Characterization, and Optical, Electrochemical Property Research of CdS/PAM Nanocomposites

Yonghong Ni,* Hequn Hao, Xiaofeng Cao, Shao Su, Yuzhong Zhang, and Xianwen Wei

College of Chemistry and Materials Science, Anhui Key Laboratory of Functional Molecular Solids, Anhui Normal University, Wuhu 241000, P.R. China

Received: March 17, 2006; In Final Form: June 11, 2006

CdS/PAM nanocomposites have been successfully synthesized in situ via a ultrasound-assisted route under ambient condition, employing $CdCl_2$ and $Na_2S_2O_3$ as Cd^{2+} and S^{2-} ion sources and acrylamide (AM) and $(NH_4)_2S_2O_8$ as organic monomers and initiating reagents, respectively. The results from X-ray powder diffraction (XRD) analysis and the IR spectrum of the final product showed the formation of CdS nanoparticles and the polymerization of AM monomers. SEM observations showed that the CdS/PAM nanocomposites could film on the quartz substrate and some holes in which many nanorods regularly arranged distributed on the film. The UV−vis absorption and PL spectra of CdS/PAM nanocomposites obviously differed from those of CdS nanoparticles prepared under the same conditions due to the presence of PAM. The electrochemical research showed that CdS/PAM nanocomposites had a stronger ability to promote electron transfers between Hb and the Au electrode than CdS nanoparticles prepared under the same conditions. A possible formation mechanism was also suggested based on the results of experiments.

1. Introduction

Over the past decade, inorganic-polymer nanocomposites have attracted much interest because of their potential applications as high-technology materials.[1−4] In polymer-based nanocomposites, the presence of inorganic nanoparticals can further modify properties of polymers due to the introduction of a second phase and a large amount of interfacial regions in these systems.[5−9] At the same time, it is necessary that the inorganic nanoparticles should be homogeneously dispersed in the polymer matrix to obtain good properties. Among various polymer-based nanocomposites, the hybridization of inorganic semiconductor nanoparticles and polymers has been the focus of intense of investigations owing to their important nonlinear properties, luminescent properties, UV-ray absorbing properties, quantum size effects, and other important physical and chemical properties.[10−14] More important, the hybridization of organic polymers and inorganic semiconductors is expected not only to permit a wide-range selection of emitter and carrier transport materials, but also to provide a new route to construct high performance electroluminescence (EL) devices through taking advantage of organic polymers and inorganic semiconductors, such as a high carrier density and a low resistivity of inorganic semiconductors and a high photoluminescent efficiency of organic polymer materials.

Many methods have been developed for the fabrication of the semiconductor/polymer nanocomposites.[15−22] However, the major disadvantages in the preparation of semiconductor−polymer nanocomposites by these methods are the poor distribution of the inorganic nanoparticle size and the poor dispersion of the inorganic particles in the polymer host. In these methods, the formations of the polymer matrix and inorganic nanoparticles are performed in two separate steps. Therefore, it is difficult to avoid both the phase separation and the aggregation of small particles.

γ-irradiation technology is probably the best method for in situ preparation of inorganic-polymer nanocomposites in one step under ambient atmosphere at room temperature.[23] However, the expensive instrument and high hazard limit its use. In recent years, the sonochemistry method attracted much attention as a new approach to prepare inorganic nanoparticles.[24] Different from other traditional chemical methods, the sonochemistry route is based on acoustic cavitations. The formation, growth, and collapse of bubbles in the liquid and the adiabatic processing of implosive collapse generate localized hot spots with transient temperatures of 5000−25000 K, pressures of ∼1800 atm,[25] and heating and cooling rates in excess of 10^{10} deg/s.[26] These extreme conditions attained during bubble collapse have been exploited to prepare amorphous metals, carbides, oxides, sulfides, etc. in various media.[24] The ultrasound preparation of metal and bimetallic nanocomposites in pure aqueous solutions was also reported.[27] However, inorganic−organic nanocomposites prepared in situ by the sonochemistry route are rarely reported in the literature.

It is well-known that CdS is a typical inorganic semiconductor material used for light-emitting diodes (LED). When it exists in a polymer matrix, the polymer is expected not only to provide good mechanical and optical properties, but also to confer a high kinetic stability on nanometer-sized semiconductor particles. In addition to the specific electronic and optical properties of CdS nanocrystals, the composite will possess excellent film processability; thus, the good optical quality thin films of the composite can be easily obtained.[21]

In this paper, we reported the in situ preparation of CdS/PAM nanocomposites via ultrasonic irradiation in an aqueous system. Compared with the traditional chemical routes, the present method did not use toxic H_2S as sulfur ion sources and all processes were carried out under the ambient conditions. Like γ-radiation technology, the formation of inorganic nanoparticles and the polymerization of monomers can be performed simultaneously. More important, the produced inorganic nano-

* Address correspondence to this author. E-mail: niyh@mail.ahnu.edu.cn.

10.1021/jp061662z CCC: $33.50
Published on Web 08/11/2006

particles can be homogeneously dispersed in polymer matrix due to the dispersion of ultrasonic waves.

2. Experimental Section

All reagents are analytically pure and used without further purification. $CdCl_2 \cdot 2.5H_2O$, $Na_2S_2O_3 \cdot 5H_2O$, $(NH_4)_2S_2O_8$, and acrylamide (AM) were purchased from ShangHai Chemical Reagent Factory, China. In a typical experiment, 0.005 mol of $CdCl_2 \cdot 2.5H_2O$ and 0.40 g of AM were dissolved in a small amount of distilled water to form 50 mL of solution; then, a little $(NH_4)_2S_2O_8$, an initiating reagent of radicals, was added to the above solution. After the mixed solution had been transferred into a 100 mL flask with a cover, the system was irradiated by 40 kHz ultrasonic waves at 100% output power. After 90 min, the fluidity of the system started to reduce, indicating that AM monomers had partly polymerized. Here, a small amount of solution containing 0.01 mol of $Na_2S_2O_3 \cdot 5H_2O$ was dropped into the above system, which was then continually ultrasonicly irradiated another 150 min. The system became yellow, sol-like, and viscous and was demulsified with absolute methanol. The yellow and viscous product was repeatedly washed with deionized water and absolute methanol several time to remove soluble inorganic salts and unreacted AM monomers. Finally, a small portion of the solution containing the product was diluted with deionized water for optical and electrochemical studies. For SEM observations a portion of the solution containing the product was expanded on a quartz flake and dried in air at room temperature. The remaining product was dried into powders in air at 60 °C for XRD and IR spectrum analyses.

As a control, pure CdS nanoparticles were also prepared under the same conditions as above.

To study the electrochemistry property of the product, dihexadecyl phosphate (DHP) was purchased from Fluka and hemoglobin from ICN Biomedicals Inc (USA). Phosphate buffer solutions (PBS; 0.1 mol/L) were prepared by mixing the stock standard solutions of K_2HPO_4 and KH_2PO_4, all containing 0.1 M NaCl. The pH values were adjusted with 0.1 mol/L H_3PO_4 or NaOH. All solutions were prepared with twice-distilled water, deoxygenated by bubbling highly pure nitrogen for 15 min, and maintained under nitrogen atmosphere during measurements at room temperature.

X-ray powder diffraction (XRD) patterns of the products were recorded on a Japan Rigaku D/max γ_A X-ray diffractometer (XRD-6000) equipped with graphite monochromatized Cu Kα radiation ($\lambda = 0.15406$ nm), using a scanning rate of 0.02 deg/s in 2θ ranges from 10° to 80°. IR spectra were obtained on a VECTORTM 22 FTIR spectrometer (Bruke, Germany). SEM images of the products were obtained from a Field emission scanning electron microananlyser (Sirion-200). TEM images were taken on a Hitachi model H-800 transmission electron microscope. The UV−vis spectra were recorded on a Hitachi U-3010 spectrophotometer (Tokyo, Japan). The fluorescence spectra were measured on a Hitachi F-2500 spectrofluorometer with a quartz cell of 1 cm. The electrochemical measurement was performed on a CHI 660A Electrochemical Workstation (CH Instruments, Chenhua Corp., Shanghai, China) with a three-electrode system consisting of a saturated calomel electrode (SCE) as a reference electrode, a platinum wire as a counter electrode, and a bare or modified Au electrode as a working electrode.

3. Results and Discussion

Although the formation of CdS can be primarily judged based on the color change of the products, to obtain convincing evidence powder X-ray diffraction was employed to analyze the phases of the products. The XRD pattern of the product is shown in Figure 1a. Three diffraction peaks at 26.5°, 44.1°, and 51.5° can be found and be indexed as (111), (220), and (311) of cubic CdS phase by comparison with the date from JCPDS No. 10-454. A broad and weak reflection peak at 2θ degrees from 14° to 24° should be attributed to the presence of the polymer. As a control, the XRD pattern of the pure CdS nanoparticles prepared from the system without AM monomers under the same experimental conditions is depicted in Figure 1b. According to Scherrer's equation, the sizes of the CdS nanoparticles are about 3 and 3.3 nm based on the (111) peak, respectively. Also, comparing with two patterns, one finds that a diffraction peak at 31.3° ((200) plane of cubic CdS) disappears in Figure 1a, which should be attributed to the influence of polymer. During the growth of crystals, the growth rate of each plane can be different due to the different adsorptions between each plane and organic or inorganic additives.[28] In this work, it was possible that an adsorption existed between PAM and CdS, which halted from the growth of CdS nanoparticles along the (200) plane. As a result, the (200) peak disappeared in Figure 1a. Nevertheless, the analyses from XRD researches indicate that CdS/PAM nanocomposites can be obtained in the system with AM monomers under the present experimental conditions.

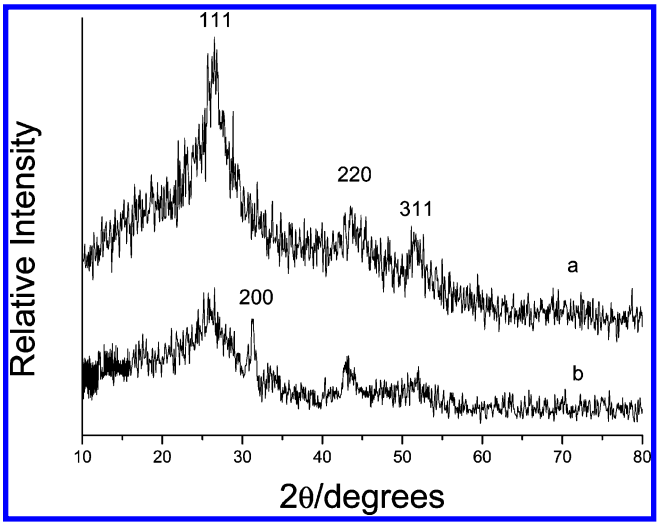

Figure 1. XRD patterns of CdS/PAM nanocomposites (a) and pure CdS nanoparticles (b) prepared under the same experiment conditions.

Also, the presence of polymer PAM in the as-prepared product can be confirmed by the IR spectrum (Figure 2). Comparing with the standard IR spectra of PAM and AM monomers,[29] one finds that the IR spectrum of the product is very close to the former, and obviously different from the latter. The strongest peaks at 3423.51 and 1657.30 cm^{-1} are ascribed to the vibration of ν_{NH} and $\nu_{C=O}$, respectively, the peaks at 2931.37 and 1453.17 cm^{-1} to the vibrations of ν_{-CH_2-} and δ_{-CH_2-}, and the peak at 1326.36 cm^{-1} to the ν_{C-C} vibration. These peaks are the characteristic peaks of PAM, which confirm that the AM monomers have successfully polymerized through the ultrasound irradiation.

SEM observations showed the CdS/PAM nanocomposite film homogeneously covered on the quartz flake. Some holes distributed on the film. A typical SEM image of the CdS/PAM nanocomposites is showed in Figure 3a. Many epitaxially grown nanorods can be found in a hole. However, the lengths and diameters of these rods are heterogeneous. The lengths range from 0.1 to 10 μm and the diameters from several 10 to several 100 nm. Furthermore, some spherical particles are also seen,

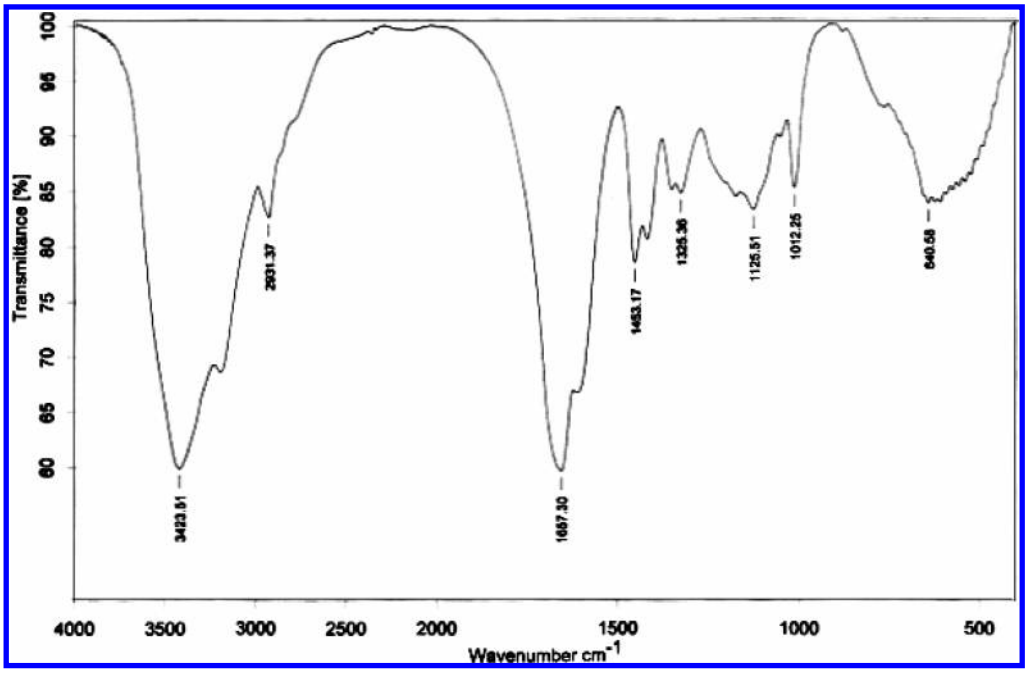

Figure 2. IR spectrum of the as-prepared CdS/PAM nanocomposites.

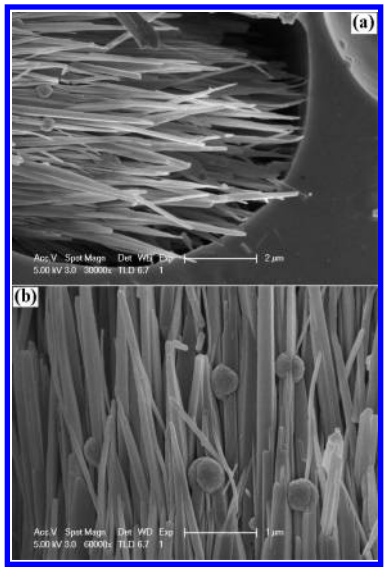

Figure 3. (a) A typical SEM image of the CdS/PAM nanocomposites in which many epitaxially grown nanorods can be found in a hole; (b) a high-resolution SEM image in which some spherical particles drilled through by the rods are also seen.

which are drilled through by the rods (see Figure 3b). To observe the distribution of CdS nanoparticles in the composites, small amounts of the nanocomposite powders were dissolved into deionized water to form a yellowish solution under ultrasound. A droplet solution was covered on the carbon-coated copper grid and dried in air. TEM observations showed that cloud-like products were the main morphology, indicating that CdS nanoparticles were very small and homogeneously dispersed in PAM (see Figure 4a, the inset is the ED pattern of the product). Also, some spherical particles with the mean diameters of ~15, ~55, and ~450 nm, and rodlike products with a mean size of 50 × 250 nm^2 could be found (see Figure 4b,c). These spherical particles should be ascribed to the aggregation of small CdS nanoparticles during the formation of the nanocomposites. In particular, the diameter of the bigger spheres was very close to that of those spheres observed in SEM images (Figure 3b). However, we did not find long and thick nanorods as shown in

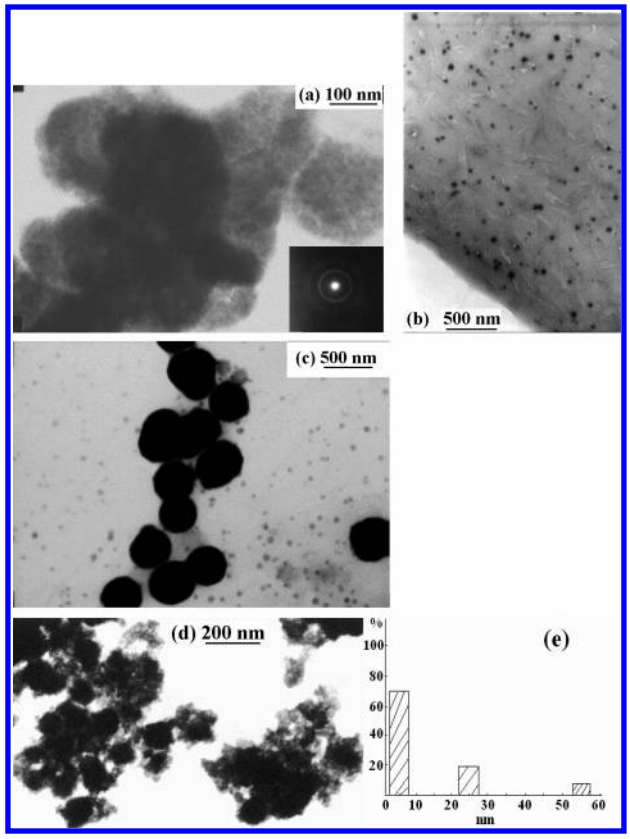

Figure 4. TEM images of the products prepared under the same experimental conditions: (a, b, and c) CdS/PAM nanocomposites, (d) pure CdS; and (e) the distribution histogram of CdS nanoparticles in the nanocomposites.

Figure 3b. This can be explained by the following possible reasons: the powders used for TEM observation were not representative or the long and thick nanorods were formed during filming of the nanocomposites. Furthermore, as a control Figure 4d depicts a TEM image of the pure CdS nanoparticels, from which the aggregation of nanoparticles is obvious. The above results indicated the polydispersive characteristic of CdS nanoparticles in the nanocomposites. A histogram of approxi-

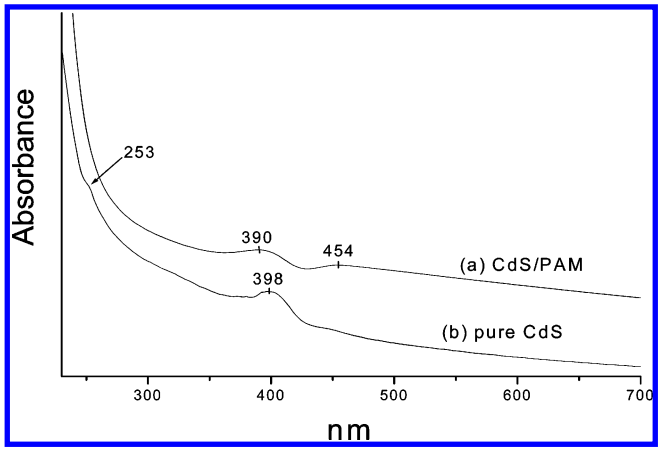

Figure 5. the UV−vis absorption spectra of the CdS/PAM nanocomposites (a) and pure CdS nanoparticles (b) prepared at the same experimental conditions.

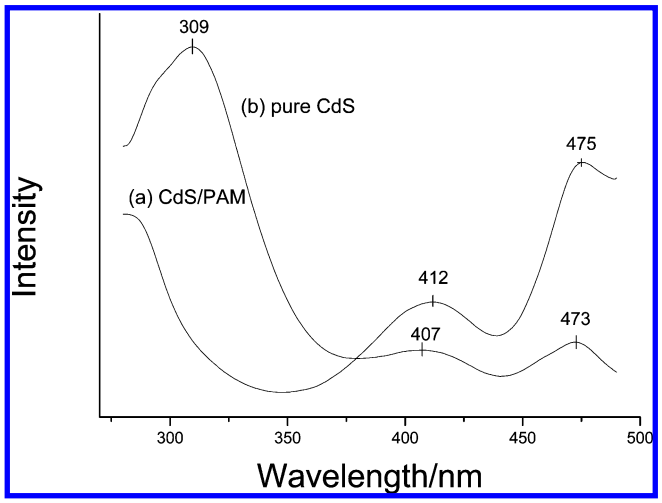

Figure 6. The PL spectra of the CdS/PAM nanocomposites and pure CdS nanoparticles prepared at the same experimental conditions, employing the exciting wavelength of 258 nm.

mative distribution of CdS nanoparticles in the nanocomposites is given in the Figure 4e based on XRD result and TEM observations.

Figure 5 shows the UV−vis absorption spectra of the CdS/PAM nanocomposites and pure CdS prepared at the same experimental conditions. A strong absorption peak at 398 nm and a weak shoulder peak at 253 nm can be seen in the absorption spectrum of pure CdS nanoparticles (Figure 5b). The strong absorption peak is assigned to the optical transition of the first excitonic state of the CdS nanoparticles,[30a] and the weak shoulder peak at 253 nm should be attributed to the multidistribution of the particle size in colloidal dispersions reported by Henglein[30b] and Yu,[30c] respectively. After the CdS/PAM nanocomposites were formed, the shoulder peak at 253 nm disappeared and a new weak peak at 454 nm appeared in the absorption spectrum of the nanocomposites (see Figure 5a). At the same time, the strong peak at 398 nm blue shifts to 390 nm, indicating that the size of CdS nanoparticles reduces in the CdS/PAM nanocomposites due to the limitation of PAM. Also, the new weak absorption at 454 nm can be ascribed to the generation of some rodlike CdS/PAM nanocomposites. A similar phenomenon is also found in PL spectra. Figure 6 is the PL spectra of the CdS/PAM nanocomposites and pure CdS prepared at the same experimental conditions, employing the exciting wavelength of 258 nm. In the PL spectrum of the pure CdS nanoparticles (Figure 6b), a strong emission peak at 309 nm

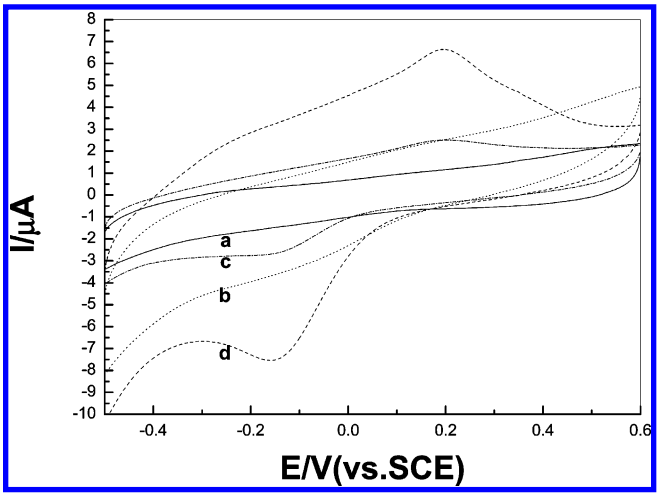

Figure 7. Cyclic voltammograms of various electrodes in 0.1 mol/L PBS at pH 6.0 at 100 mV·s^{-1}: (a) bare Au or Hb/Au, (b) CdS-PAM nanocomposites/Au, (c) Hb/CdS-PAM nanocomposites/Au, and (d) DHP/Hb/CdS-PAM nanocomposites/Au.

and two weak emission peaks at 407 and 473 nm can be easily seen. However, in that of the CdS/PAM nanocomposites the strong peak at 309 nm disappears and two weak peaks enhance and shift to 412 and 475 nm, respectively. Here, the strong peak at 309 nm is ascribed to the Stocks shift peak based on the result of experiments; the emission peak at ~400 nm arose from the recombination of excitrons and/or shallowly trapped electron−hole pairs;[31a] and the peak at about 475 nm was attributed to the intrinsic character of CdS nanoparticles, which had been reported by Butty et al.[31b] The above experimental results adequately illuminate that the presence of PAM can strongly influence the optical property of CdS nanoparticles.

Also, the electrochemistry property of the as-prepared CdS/PAM nanocomposites was studied. The cyclic voltammograms of different electrodes in 0.1 mol/L phosphate buffer solution (PBS) (pH 6.0) are shown in Figure 7. No redox peak is observed when a bare Au electrode is used (curve a). Since hemoglobin (Hb) hardly shows a pair of redox peaks at solid electrodes,[32] no change is found with use of a Hb-modified Au electrode. There are no redox peaks with only the Au electrode modified with CdS/PAM nanocomposites (curve b), but a couple of distinct redox peaks were displayed employing a Hb/CdS-PAM nanocomposites modified Au electrode (curve c). The oxidation and reduction peak potentials are 195 mV and −114 mV, respectively. The above phenomenon implies that the as-prepared CdS/PAM nanocomposites can improve the electron transfer between Hb and the Au electrode. Moreover, the electron transfer between Hb and the Au electrode was further promoted when a surfactant, dihexadecyl phosphate (DHP), was cast on the Hb/CdS-PAM nanocomposites/Au electrode (curve d). However, the main contribution should also be ascribed to the presence of CdS/PAM nanocomposites, because further research indicated that only a weak reduction peak appeared with use of a DHP/Hb modified Au electrode (see Figure 8, curve a). At the same time, research still found that the presence of PAM could obviously have an affect on the electrochemical property of CdS nanoparticles. Figure 8b is the current−voltage curve recorded with a DHP/Hb/CdS nanoparticles modified Au electrode. A couple of weak redox peaks are displayed, indicating that CdS nanoparticles can promote the electron transfer between Hb and the Au electrode. After CdS nanoparticles were substituted with CdS/PAM nanocomposites, the promotion of electron transfers between Hb and the Au electrode was greatly enhanced (Figure 8, curve c), implying that CdS/

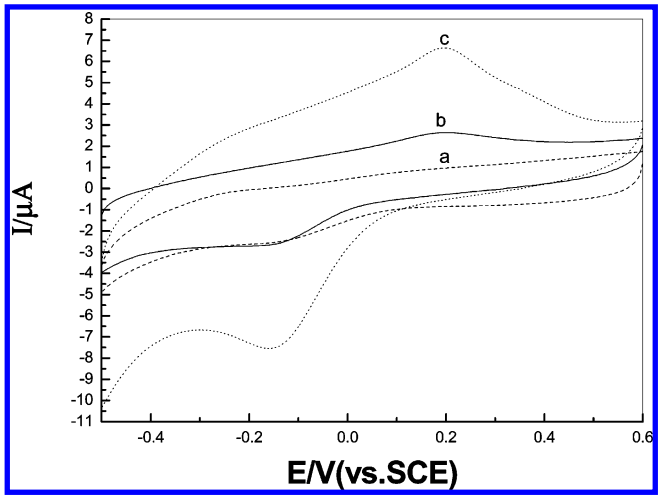

Figure 8. Cyclic voltammograms of various electrodes in 0.1 mol/L PBS at pH 6.0 at 100 $mV \cdot s^{-1}$: (a) DHP/Hb/Au, (b) DHP/Hb/CdS nanoparticles/Au, and (c) DHP/Hb/CdS-PAM nanocomposites/Au.

PAM nanocomposites have a better electrochemical property than CdS nanoparticles prepared under the same experimental conditions.

The formation mechanism of sulfide nanoparticles under ultrasonic irradiation has been extensively studied in the aqueous system.[33] The general opinion is that the formation of sulfide nanoparticles is probably related to the radical species generated from water molecules by the absorption of the ultrasonic energy. It has been known that during an aqueous sonochemical process, the elevated temperatures and pressures inside the collapsing bubbles cause water molecules to vaporize and further pyrolyze into $H^{\bullet}$ and $^{\bullet}OH$ radicals.[33a] The $H^{\bullet}$ radicals are reductive particles, which can reduce the sulfur source into S^{2-} ions. The produced S^{2-} ions rapidly react with metal cations such as Cd^{2+} to form CdS nanoparticles. In our work, an inducing reagent $(NH_4)_2S_2O_8$ was introduced into the system for easier polymerization of AM monomers. Since $(NH_4)_2S_2O_8$ is also an oxidant and can be spent by $Na_2S_2O_3$, no CdS/PAM nanocomposites were obtained when $(NH_4)_2S_2O_8$ and $Na_2S_2O_3$ were added to the system simultaneously. To prepare CdS/PAM nanocomposites successfully, AM monomers were prepolymerized via the initiation of $(NH_4)_2S_2O_8$ during the experiments. Then, $Na_2S_2O_3$ was added to the solution. After successive ultrasonic irradiation for a period of time, CdS/PAM nanocomposites were obtained. The above processes can be described with equations as follows:

$$H_2O \rightarrow H^{\bullet} + {}^{\bullet}OH \quad (1)$$

$$S_2O_3^{2-} + 2H^{\bullet} \rightarrow S^{2-} + 2H^{+} + SO_3^{2-} \quad (2)$$

$$S^{2-} + Cd^{2+} \rightarrow CdS \quad (3)$$

$$S_2O_8^{2-} \rightarrow 2SO_4^{\bullet -} \quad (4)$$

$$AM + NH_4SO_4^{\bullet} \rightarrow PAM \quad (5)$$

The total reaction is

$$Cd^{2+} + S_2O_3^{2-} + AM \rightarrow \text{CdS/PAM nanocomposites}$$

4. Conclusion

CdS/PAM nanocomposites have been successfully prepared in situ by ultrasound irradiation in an aqueous system under ambient atmosphere. Compared with pure CdS nanoparticles prepared under the same experimental conditions, CdS/PAM nanocomposites had better electrochemical property. On the other hand, there are distinct differences in the photoluminescence and UV−vis spectra of the pure CdS and CdS/PAM nanocomposites, which should be attributed to the influence of polymer PAM. More important, the as-prepared CdS/PAM nanocomposites have good film processability, which is availed to application of CdS/PAM nanocomposites. Furthermore, this method can also be used for the preparation of other metal sulfide−polymer nanocomposites.

Acknowledgment. The authors thank the National Natural Science Foundation of China (20571002), the Natural Science Foundation of Anhui Province (05021024), the Education Department of Anhui Province (2005kj123 and No. 2006KJ006TD), and the special fund of Anhui Normal University (2005xzx17) for fund support. Prof. X. W. Wei thanks the Anhui Provincial Excellent Young Scholars Foundation (No. 04046065) for fund support.

References and Notes

(1) Chang, L. T.; Yen, C. C. *J. Appl. Polym. Sci.* **1995**, *55*, 371.
(2) Alivisatos, A. P. *Science* **1996**, *273*, 933.
(3) Beecroft, L. L.; Ober, C. K. *Chem. Mater.* **1997**, *9*, 1302.
(4) Antonietti, M. *Adv. Mater.* **1998**, *10*, 195.
(5) Ki, J. U.; Shanghnessy, B. O. *Phys. Rev. Lett.* **2002**, *89*, 238301.
(6) Mukherjee, M.; Dutta, A.; Chakravorty, D. *Appl. Phys. Lett.* **1994**, *64*, 1159.
(7) Cole, D. H.; Shull, K. R.; Rehn, L. E.; Baldo, P. *Phys. Rev. Lett.* **1997**, *78*, 5006.
(8) Mukherjee, M.; Chakravorty, D.; Nambissan, P. M. G. *Phys. Rev. B* **1998**, *57*, 848.
(9) Mustarelli, P.; Capiglia, C.; Quartarone, E.; Tomasi, C.; Ferloni, P.; Linati, L. *Phys. Rev. B* **1999**, *60*, 7228.
(10) Heron, N.; Calabrese, J. C.; Farneth, W. E.; Wang, Y. *Science* **1993**, *259*, 1426.
(11) Henshaw, G.; Parkin, I. P.; Shaw, G. *J. Chem. Soc., Chem. Commun.* **1996**, 1095.
(12) Brus, L. E. *Appl. Phys. A* **1991**, *53*, 456.
(13) Rossetti, R.; Hull, R.; Gibson, J. M.; Brus, L. E. *J. Chem. Phys.* **1995**, *82*, 552.
(14) Henglein, A. *Chem. Rev.* **1989**, *89*, 1861.
(15) Meissner, D.; Memming, R.; Kastening, B. *Chem. Phys. Lett.* **1983**, *96*, 34.
(16) Krishnan, M.; White, J. R.; Fox, M. A.; Bard, A. *J. Am. Chem. Soc.* **1983**, *105*, 7002.
(17) Huang, J. M.; Yang, Y.; Yang, B.; Liu, S. Y.; Shen, J. C. *Polym Bull.* **1996**, *36*, 337.
(18) Gao, M. Y.; Xi, Z.; Yang, B.; Shen, J. C. *J. Chem. Soc., Chem. Commun.* **1994**, 2229.
(19) Huang, J. M.; Yang, Y.; Yang, B.; Liu, S. Y.; Shen, J. C. *Polym. Bull.* **1996**, *37*, 679.
(20) Wang, Y.; Herron, N. *Chem. Phys. Lett.* **1992**, *200*, 71.
(21) Yang, Y.; Xue, S.; Liu, S.; Huang, J.; Shen, J. *Appl. Phys. Lett.* **1996**, *69*, 377.
(22) Zhou, Y.; Hao, L.; Yu, S.; You, M.; Zhu Y.; Chen, Z. *Chem. Mater.* **1999**, *11*, 3411.
(23) (a) Ni, Y.; Ge, X.; Liu, H.; Zhang, Z.; Ye, Q.; Wang, F. *Chem. Lett.* **2001**, *5*, 458. (b) Ni, Y.; Ge, X.; Zhang, Z. *Mater. Lett.* **2002**, *55*, 171. (c) Ni, Y.; Ge, X.; Zhu, Z.; Zhang, Z. *J. Chem. Phys.* (*China*) **2002**, *15*, 393. (d) Ni, Y.; Ge, X.; Liu, H.; Zhang, Z.; Ye, Q. *Chem. Lett.* **2001**, *9*, 924. (e) Ni, Y.; Ge, X.; Zhang, Z. *Mater. Sci. Eng. B* **2005**, *119*, 51.
(24) (a) Wang, G.; Geng, B.; Huang, X.; Wang, Y.; Li, G.; Zhang, L. *Appl. Phys. A* **2003**, *77*, 933. (b) Yin, J. L.; Qian, X.; Yin, J.; Shi, M.; Zhou, G. *Mater. Lett.* **2003**, *57*, 3859. (c) Wang, H.; Lu, Y.; Zhu, J.; Chen, H. *Inorg. Chem.* **2003**, *42*, 6404. (d) Zhang, J.; Chen, Z.; Wang, Z.; Ming, N. *J. Mater. Res.* **2003**, *18*, 1804. (e) Gedanken, A. *Ultrason. Sonochem.* **2004**, *11*, 47 and references cited in this paper.
(25) (a) Suslick, K. S.; Choe, S.-B.; Cichowlas, A. A.; Grinstaff, M. W. *Nature* **1991**, *353*, 414. (b) Suslick, K. S.; Hammerton, D. A.; Cline, R. E. *J. Am. Chem. Soc.* **1986**, *108*, 5641.
(26) (a) Barber, B. P.; Putterman, S. J. *Nature* **1991**, *352*, 414. (b) Hiller, R.; Putterman, S. J.; Barber, B. P. *Phys. Rev. Lett.* **1992**, *69*, 1182.
(27) Oshima, R.; Yamamoto, T. A.; Mizukoshi, Y.; Nagata, Y.; Meada, Y. *Nanostruct. Mater.* **1999**, *111*, 12.

(28) (a) Buckley, H. E. *Crystal Growth*; Wiley: New York, 1951. (b) Siegfried, M. J.; Choi, K. S. *Adv. Mater*. **2004**, *16*, 1743.

(29) Sprouse, J. F. *Sprouse Collection of Infrared Spectra Book I: Polymers*, No. 357; Sprouse Scientific Systems, Inc.: Paoli, PA, 1987. *Standard Infrared Grating Spectra*, Vols. 9−10 (8001−10000), Sadtler Research Laboratories, Division of Bio-Rad Laboratories, Inc. USA, 1980; No. 8112.

(30) (a) Weller, H. *Angew. Chem., Int. Ed.* **1993**, *32*, 41. (b) Henglein, A. In *Modern Trends of Colloid Science in Chemistry and Biology*; Eicka, H. F., Ed.; Birkhauser: Basel, 1985. (c) Yu, W. L.; Pei, J.; Huang, W.; Zhao, G. X. *Mater. Chem. Phys.* **1997**, *49*, 87.

(31) (a) Chen, W.; Wang, Z. G.; Lin, Z. J.; Lin, L. Y. *Solid State Commun.* **1997**, *101*, 371. (b) Butty, J.; Peyghambarian, N. *Appl. Phys. Lett.* **1996**, *69*, 3224.

(32) Wang, L.; Hu, N. *Bioelectrochemistry* **2001**, *53*, 205.

(33) (a) Wang, H.; Zhu, J. J. *Ultrason. Sonochem.* **2004**, *11*, 293. (b) Wang, G.; Chen, W.; Liang, C.; Wang, Y.; Meng, G.; Zhang, L. *Inorg. Chem. Commun*. **2001**, *4*, 208.